

New BODIPY lipid probes for fluorescence studies of membranes

Ivan A. Boldyrev,^{1,*} Xiuhong Zhai,^{1,†} Maureen M. Momsen,[†] Howard L. Brockman,[†] Rhoderick E. Brown,^{2,†} and Julian G. Molotkovsky^{2,*}

Shemyakin and Ovchinnikov Institute of Bioorganic Chemistry,* Russian Academy of Sciences, Moscow, 117997 Russia; and Hormel Institute,[†] University of Minnesota, Austin, MN 55912

Abstract Many fluorescent lipid probes tend to loop back to the membrane interface when attached to a lipid acyl chain rather than embedding deeply into the bilayer. To achieve maximum embedding of BODIPY (4,4-difluoro-4-bora-3a,4a-diaza-s-indacene) fluorophore into the bilayer apolar region, a series of *sn*-2 acyl-labeled phosphatidylcholines was synthesized bearing 4,4-difluoro-1,3,5,7-tetramethyl-4-bora-3a,4a-diaza-s-indacene-8-yl (Me₄-BODIPY-8) at the end of C₃, C₅, C₇, or C₉-acyl. A strategy was used of symmetrically dispersing the methyl groups at BODIPY ring positions 1, 3, 5, and 7 to decrease fluorophore polarity. Iodide quenching of the phosphatidylcholine probes in bilayer vesicles confirmed that the Me₄-BODIPY-8 fluorophore was embedded in the bilayer. Parallax analysis of Me₄-BODIPY-8 fluorescence quenching by phosphatidylcholines containing iodide at different positions along the *sn*-2 acyl chain indicated that the penetration depth of Me₄-BODIPY-8 into the bilayer was determined by the length of the linking acyl chain. Evaluation using monolayers showed minimal perturbation of <10 mol% probe in fluid-phase and cholesterol-enriched phosphatidylcholine. Spectral characterization in monolayers and bilayers confirmed the retention of many features of other BODIPY derivatives (i.e., absorption and emission wavelength maxima near 498 nm and ~506–515 nm) but also showed the absence of the 620–630 nm peak associated with BODIPY dimer fluorescence and the presence of a 570 nm emission shoulder at high Me₄-BODIPY-8 surface concentrations. **■** We conclude that the new probes should have versatile utility in membrane studies, especially when precise location of the reporter group is needed.—Boldyrev, I. A., X. Zhai, M. M. Momsen, H. L. Brockman, R. E. Brown, and J. G. Molotkovsky. **New BODIPY lipid probes for fluorescence studies of membranes.** *J. Lipid Res.* 2007. 48: 1518–1532.

Supplementary key words spectral properties • monolayers • lipid lateral packing • surface compressional modulus • lipid phase state • fluorophore position • fluorescence quenching • iodide • fluorophore location in bilayers • parallax analysis • 4,4-difluoro-4-bora-3a,4a-diaza-s-indacene

Manuscript received 18 October 2006 and in revised form 19 March 2007.
Published, JLR Papers in Press, April 7, 2007.
DOI 10.1194/jlr.M600459-JLR200

Fluorescent lipid probes have proven to be valuable tools in membrane studies (see Ref. 1 for review). Because the determination of depth-dependent parameters of bilayers can benefit the understanding of membranous structures (2), sets of probes bearing the same fluorophore at different distances from the bilayer surface are potentially quite useful. Ideally, such fluorophores should be apolar enough to localize at the membrane depth that reflects the apolar nature of the surrounding acyl chain region without being strongly influenced by the trans-bilayer polarity gradient (3). The first probe set designed to achieve this goal was a series of *n*-(9-anthroyloxy) fatty acids synthesized by Thulborn and Sawyer (4), who showed that the fluorophore resided in the bilayer at a graded series of depths that coincided with the attachment point of the anthroyloxy fluorophore along the acyl chain. Other widely used fluorophores, such as *N*-dansyl (5) or *N*-NBD (6, 7), have been shown to have polar characteristics that interfere with localization deep inside the bilayer even when attached to the end of the acyl chain.

During the past decade, BODIPY (4,4-difluoro-4-bora-3a,4a-diaza-s-indacene) fluorophore probes have found a wide range of applications in cell biology and biophysics, even though this zwitterionic fluorophore was first synthesized by Treibs and Kreuzer (8) in 1968. The BODIPY fluorophore family has gained popularity because of its overall excellent spectral properties (9, 10), which include high photostability, high molar absorptivities, high quantum yields, and strong, narrow-wavelength emission max-

Abbreviations: AV12-PC, 1-acyl-2-[12-(9-anthryl)-11*E*-dodecenoyl]-*sn*-glycero-3-phosphocholine; B3-, B5-, B7-, or B9-PC, phosphatidylcholine bearing at the *sn*-2 position ω -Me₄-BODIPY-8-C₃-, -C₅-, -C₇-, or -C₉-fatty acid, respectively; DMPC, 1,2-dimyristoyl-*sn*-glycero-3-phosphocholine; I7- or I11-PC, phosphatidylcholine bearing 7-iodoheptanoic or 11-iodoundecanoic acid, respectively, at the *sn*-2 position; *K*_{sv}, Stern-Volmer quenching constant; Me₂-BODIPY-3, 4,4-difluoro-5,7-dimethyl-4-bora-3a,4a-diaza-s-indacene-3-yl; Me₄-BODIPY-8, 4,4-difluoro-1,3,5,7-tetramethyl-4-bora-3a,4a-diaza-s-indacene-8-yl; PB-PC, 1-palmitoyl-2-Me₂-BODIPY-3-pentanoyl-*sn*-glycero-3-phosphocholine; *T*_m, phase transition temperature.

¹I. A. Boldyrev and X. Zhai contributed equally to this work.

²To whom correspondence should be addressed.

e-mail: reb@umn.edu (R.E.B.); jgmol@ibch.ru (J.G.M.)

ima in the visible region. Although the great majority of BODIPY fluorophores are nearly insensitive to environmental polarity and this property is advantageous for many applications, a few environmentally responsive varieties of BODIPY have been developed (11). Many BODIPY derivatives, including labeled fatty acids and complex lipid probes, have been synthesized (12, 13) and applied in numerous biological studies (1, 14). These probes are commercially available (Invitrogen) (15) but are relatively expensive, presumably because of their rather complicated syntheses.

Because the BODIPY group carries no net charge, one might expect it to be a more reliable depth-dependent membrane probe than dansyl or NBD. Despite the seemingly favorable properties, studies of the localization of lipid-attached BODIPY in model membranes have led to conflicting conclusions. Based on iodide quenching studies of different BODIPY probes in phospholipid vesicles and in water, Johnson, Kang, and Haugland (9) concluded that lipid-attached BODIPY fluorophores reside mainly in the bilayer at the expected depth. On the other hand, Menger, Keiper, and Caran (16), using spin-labeled lipids as quenchers incorporated into the membrane, found that BODIPY fluorophores linked to various positions of the phosphatidylcholine acyl chain, including the ω position, reside close to the membrane surface, ~ 17 – 20 Å from the bilayer center, as determined by parallax analysis. However, Kaiser and London (17), also using spin-labeled lipid quenchers and parallax analysis, concluded that lipid-attached BODIPY in the bilayer distributes between two populations: in one, the fluorophore is embedded into bilayer along the entire length of the acyl chain; in the other population, BODIPY resides closer to the membrane surface by causing bending/looping of the flexible acyl chain. Even though such dual fluorophore localization and related uncertainties do not diminish the effectiveness of BODIPY for many purposes (e.g., monitoring lipid trafficking within a cell), it can be problematic in other cases, such as in resonance energy transfer experiments in which the fluorophore serves as a molecular ruler, thus requiring its membrane position to be accurately known.

The goal of this study was to develop a set of lipid probes, bearing a BODIPY fluorophore at the end of the acyl chain, in which the fluorophore location within the bilayer corresponded to the maximal depth allowed by the acyl chain. Our strategy was to modify the BODIPY structure to counteract the polarity originating from its compensating positive (on nitrogen atom) and negative (on boron atom) internal charges to optimize its capacity for localization in the apolar interior of the bilayer. As a rule, insertion of substituents at positions 1, 3, 5, 7, and 8 of the BODIPY ring (Fig. 1), but not at positions 2 and 6, is known to be well tolerated without negatively affecting emission quantum yield (9). It should be noted that the previously described studies of lipid-bonded BODIPY localization in bilayers (9, 16, 17) were performed using fluorophore containing methyl substituents at positions 5 and 7 and linked to acyl chains via position 3. We rea-

soned that BODIPY could be optimized for deep bilayer localization by maximizing the number and symmetry of apolar substituents. Our considerations led to the hypothesis that the desired fluorophore should have the BODIPY ring, with identical apolar alkyls at positions 1, 3, 5, and 7, and be linked to acyl chains via position 8. To evaluate this hypothesis, we analyzed the spectral and membrane properties of BODIPY probes with the aforementioned structural features, 4,4-difluoro-1,3,5,7-tetramethyl-4-bora-3a,4a-diaza-*s*-indacene-8-yl ($\text{Me}_4\text{-BODIPY-8}$). For this purpose, a novel set of phosphatidylcholines was synthesized with the $\text{Me}_4\text{-BODIPY-8}$ fluorophore attached to the end of *sn*-2 fatty acids consisting of three, five, seven, or nine carbon atoms. The location and insertion depth of the $\text{Me}_4\text{-BODIPY-8}$ fluorophore in unilamellar bilayer vesicles have been assessed by quenching with free iodide (Stern-Volmer analysis) as well as with iodolabeled phosphatidylcholines (parallax analysis) (17). The physical and spectral features of these new phosphatidylcholine probes, in their pure states and in mixtures with other lipids, have been characterized in both bilayer and monolayer model membrane systems to assess the occurrence of lipid-packing distortions caused by the fluorophore as well as concentration-dependent dimerization associated with the BODIPY family of fluorophores (18, 19).

MATERIALS AND METHODS

Materials

1,2-Dimyristoyl-*sn*-glycero-3-phosphocholine (DMPC), POPC, cholesterol, and sodium PBS (10 mM, pH 7.4, in 150 mM NaCl and 1 mM EDTA) were purchased from the Sigma Chemical Co. 1-Palmitoyl-2- $\text{Me}_2\text{-BODIPY-3-pentanoyl-}sn\text{-glycero-3-phosphocholine}$ (PB-PC; Fig. 1) was from Invitrogen. 1-Acyl-2-[12-(9-anthryl)-11*E*-dodecenoyl]-*sn*-glycero-3-phosphocholine (AV12-PC; Fig. 1) was prepared as described previously (5). Other phosphatidylcholines were from Avanti Polar Lipids (Alabaster, AL). The syntheses of the $\text{Me}_4\text{-BODIPY-8}$ -labeled probes (20) are summarized in the scheme (Fig. 1). The synthesis of phosphatidylcholine bearing 7-iodoheptanoic or 11-iodoundecanoic acid at the *sn*-2 position (I7-PC or I11-PC; Fig. 1) will be reported elsewhere (21).

Vesicle preparation

An aliquot of lipid solution in chloroform was rotary-evaporated in a round-bottomed flask and kept in vacuo (20 Pa) for 2 h. The resulting lipid film was suspended in PBS at the desired lipid concentration (400 $\mu\text{g}/\text{ml}$) and subjected to 10 cycles of freezing (liquid nitrogen) and thawing (water bath at 40°C for POPC and at 50°C for DMPC or DMPC/cholesterol). Then, the lipid suspension was extruded through polycarbonate membranes (Nucleopore) with 100 nm pores 20 times using the mini-extruder (Avanti Polar Lipids). The resulting vesicles, as shown previously (22), are unilamellar with mean diameters of ~ 120 nm.

Spectral measurements

The UV spectra were recorded on an Ultrospec II spectrophotometer (Pharmacia LKB, Bromma, Sweden). Steady-state fluorescence measurements were performed on an F-4000

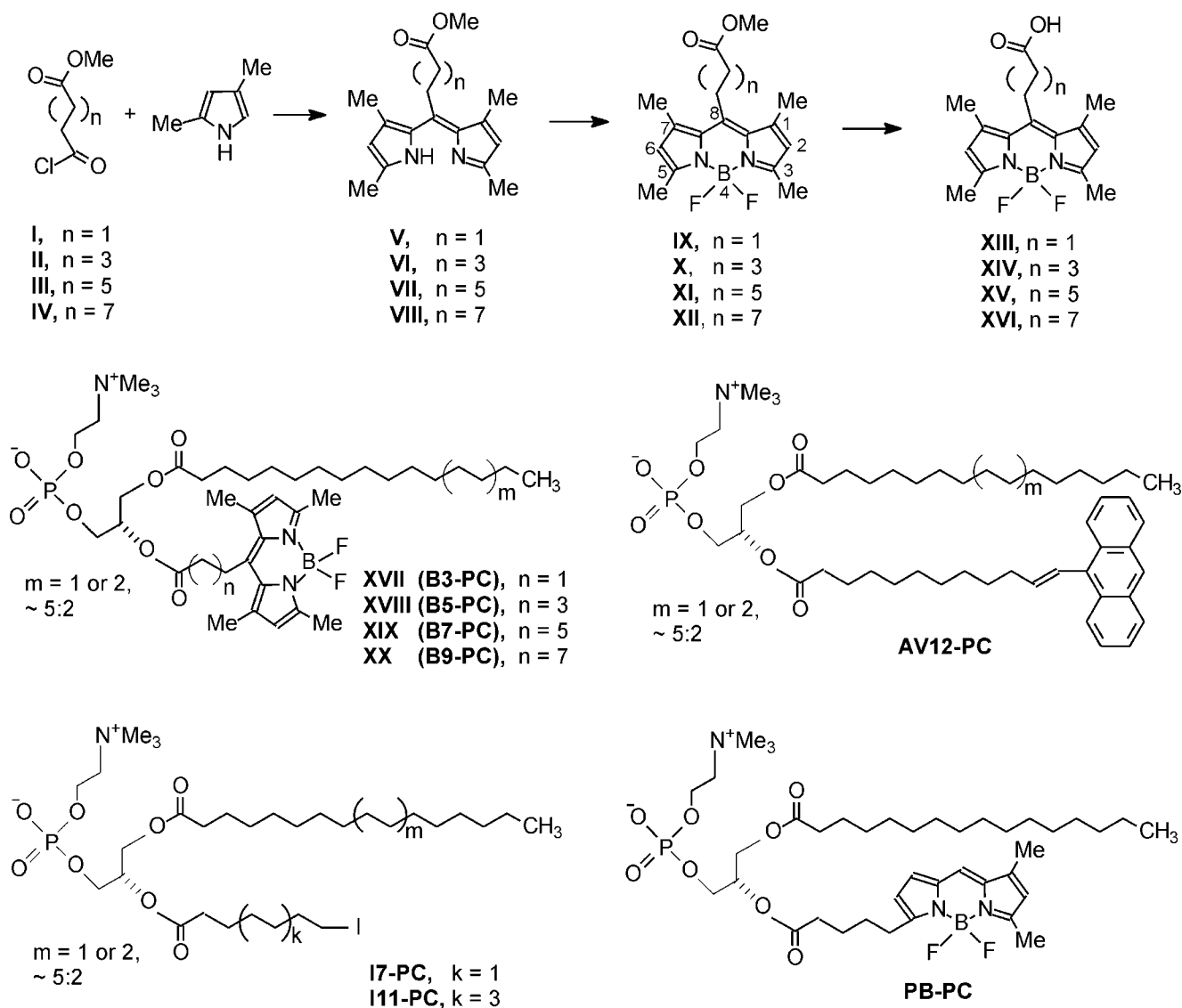


Fig. 1. Synthesis of acids XIII–XVI, and structures of 4,4-difluoro-1,3,5,7-tetramethyl-4-bora-3a,4a-diaza-s-indacene-8-yl ($\text{Me}_4\text{-BODIPY-8}$), AV12-PC, $\text{Me}_2\text{-BODIPY-3}$, and iodolabeled probes. AV12-PC, 1-acyl-2-[12-(9-anthryl)-11*E*-dodecenoyl]-*sn*-glycero-3-phosphocholine; B3-, B5-, B7-, or B9-PC, phosphatidylcholine bearing at the *sn*-2 position $\omega\text{-Me}_4\text{-BODIPY-8-C}_3\text{-}$, $\text{-C}_5\text{-}$, $\text{-C}_7\text{-}$, or $\text{-C}_9\text{-}$ fatty acid, respectively; I7- or I11-PC, phosphatidylcholine bearing 7-iodoheptanoic or 11-iodoundecanoic acid, respectively, at the *sn*-2 position; PB-PC, 1-palmitoyl-2- $\text{Me}_2\text{-BODIPY-3-pentanoyl-}$ *sn*-glycero-3-phosphocholine.

fluorimeter (Hitachi, Ltd., Tokyo, Japan) using thermostatted 10×10 mm cuvettes. $\text{Me}_4\text{-BODIPY-8}$ probes were excited at 497 nm, unless specified otherwise, and the emission was recorded at 505 nm using excitation and emission band passes of 5 nm. Anthrylvinyl probe was excited at 373 nm, and the emission was recorded at 434 nm (excitation and emission band passes of 5 and 10 nm, respectively). In the liposome experiments, a cross-oriented configuration of the polarizers ($\text{Ex}_{\text{pol}} = 0^\circ$ and $\text{Em}_{\text{pol}} = 90^\circ$) was used for maximal suppression of liposome-scattering side effects (23). Fluorescence of high-concentration probe solution (5% in chloroform) was measured in three sealed glass capillaries (inner diameter, 0.5 mm) placed cornerwise in a quartz cuvette filled with toluene to minimize light reflection at the external surface of the capillaries.

In iodide quenching experiments involving $\text{Me}_4\text{-BODIPY-8}$ probes (0.1 mol% total lipid) and AV12-PC (0.5 mol% total lipid) in vesicles (0.4 mg lipid/ml), the data were collected by

sequential addition of the stock quencher solution (1.5 M sodium iodide containing 10 mM $\text{Na}_2\text{S}_2\text{O}_3$ in PBS) to vesicles containing the probe and subsequent measurement of fluorescence intensity after system equilibration (up to 60 min) similar to our previous studies (24, 25). During the quenching experiments, osmolarity changes caused by the addition of iodide salts to the suspension, apart from dilution, can bring about vesicle swelling and change the relative refractive index at the solution/vesicle boundary. Because both effects can influence vesicle turbidity (26, 27), steps were taken to correct for their contributions to the emission quenching data by performing parallel control measurements in which equal aliquots of 1.5 M sodium chloride solution in PBS were added to vesicle samples instead of quencher solution.

For Stern-Volmer plots, F_0/F values were calculated as follows:

$$F_0/F = F_0/F^q - F_0/F^c + 1 = 1 + K_{sv}[Q] \quad (\text{Eq. 1})$$

where F_0 , F^q , and F^c are emission intensities of unquenched, quenched, and control samples, respectively, K_{sv} is the Stern-Volmer quenching constant, and $[Q]$ is the quencher concentration. Equation 1 is derived in the following way. The observed emission change in response to quencher addition, F_0/F^q , may be presented as a sum of the genuine effect of quencher F_0/F and some corrective function $f(d)$, which compensates for dilution and the other mentioned side effects:

$$F_0/F^q = F_0/F + f(d) \quad (\text{Eq. 2})$$

To estimate $f(d)$, measurements are made on vesicles using an appropriate quencher substitute, such as NaCl solution. Then, the process should follow the Stern-Volmer rule:

$$F_0/F^c = 1 + f(d) \quad (\text{Eq. 3})$$

Combining equations 2 and 3 gives equation 1.

For quenching experiments with iodolabeled phosphatidylcholines, POPC vesicles containing 5 mol% I7- or I11-PC and a Me₄-BODIPY-8 probe (0.1 mol%) were prepared as described above. To avoid inner filter effects, total absorbance was kept low (~ 0.02 at 498 nm). The distance of the fluorophore from the center of the bilayer was calculated using the parallax equation (17, 28):

$$z_{CF} = L_{C1} + [-\ln(F_1/F_2)/\pi \times C - L_{21}^2]/2L_{21} \quad (\text{Eq. 4})$$

where z_{CF} is the distance of the fluorophore from the bilayer center, F_1 is the relative fluorescence intensity (F/F_0) in the presence of shallow quencher (quencher 1, I7-PC), F_2 is the relative fluorescence intensity (F/F_0) in the presence of deeper quencher (quencher 2, I11-PC), L_{C1} is the distance of the shallow quencher from the bilayer center, L_{21} is the distance between shallow and deep quenchers, and C is the quencher concentration in mole fraction of quencher/area per phospholipids (assuming 70 Å² per POPC molecule). Distances of the iodine atoms from the bilayer center, 8.8 ± 2.3 Å for I7-PC and 5.8 ± 2.9 Å for I11-PC (assuming that the iodine atoms reside at positions C-8 and C-12 of the *sn*-2-acyl, correspondingly, in the phosphatidylcholine molecule), as well as the corresponding distances for fluorophores were calculated on the basis of the 200 molecule fluid POPC bilayer model (29).

Monolayer conditions

The monolayer properties of the lipid probes, in pure form and mixed with other lipids, were characterized using a computer-controlled, Langmuir-type film balance designed to measure the surface pressure (π) and dipole potential (ΔV) as a function of cross-sectional molecular area (A) while simultaneously acquiring the fluorescence emission intensity as a function of wavelength at the desired surface pressures. Surface pressure and area calibration of the film balance were performed as detailed previously (30, 31). Fluorescence emission measurements were performed using a slightly modified set-up compared with that described by Dahim et al. (32). Briefly, BODIPY lipid films were excited at a 90° incident angle using 488 nm unpolarized light from an argon-ion laser (model 2122-45L; JDS Uniphase, San Jose, CA) equipped with a model-3 light-intensity controller and a fiber-optic coupler (model HPUC-23-488-S-3, FAC-2BL; Oz Optics, Nepean, Ontario, Canada). Fluorescence emission was collected perpendicular to the interface at a distance of ~ 1 cm using a fiber-optic spectrometer (model PC2000-ISA; Ocean Optics, Dunedin, FL) equipped with an L2 lens and a 200 μm slit. A 500 nm long-pass filter (500EFLP; Omega Optical, Brattleboro, VT) was mounted between the emission collimator and the detector to reduce scattered excitation light. Fluores-

cence emission spectral intensities were collected each second. Although monolayer compression was continuous during the spectral data acquisition cycle, the fractional change in lipid concentration during each acquisition cycle was ≤ 0.0073 . Emission spectra were not affected by gas phase (i.e., air or argon) or by 0.01% sodium azide in the subphase buffer.

Lipid monolayers were formed by spreading (51.67 μl aliquots) mixtures made from stock solutions dissolved in toluene-ethanol (5:6) or hexane-isopropanol-water (70:30:2.5). Solvent purity was verified by dipole potential measurements using a ²¹⁰Po ionizing electrode (31). After spreading on the subphase surface, lipid films were compressed at a rate of ≤ 4 Å²/molecule/min after a delay period of 4 min. Subphase buffer was maintained at 24°C via a thermostatted, circulating water bath and was produced using water previously purified by reverse osmosis, activated charcoal adsorption, and mixed-bed deionization, then passed through a Milli-Q UV Plus system (Millipore Corp., Bedford, MA) and filtered through a 0.22 μm Millipak 40 membrane. Subphase buffer contained 10 mM potassium phosphate (pH 6.6), 100 mM NaCl, and 0.2% NaN₃ and was kept stored under argon, which was cleaned by passage through a seven stage series filtration set-up consisting of an Alltech activated charcoal gas purifier, a LabClean filter, and a series of Balston disposable filters consisting of two adsorption (carbon) units and three filter units (93% and 99.99% efficiency at 0.1 μm). The film balance was housed in an isolated laboratory supplied with clean air by a Bioclean air filtration system equipped with charcoal and High Efficiency Particulate Air (HEPA) filters and was kept under humidified argon in a separate enclosure. Other features contributing to isotherm reproducibility include automated lipid spreading via a modified HPLC autoinjector, automated surface cleaning by multiple barrier sweeps between runs, and highly accurate, reproducible setting of the subphase level by an automated aspirator. Glassware was acid-cleaned and rinsed with purified water and then with hexane-ethanol (95:5) before use.

Analyses of Monolayer Isotherms

The dipole potential versus cross-sectional molecular area ($\Delta V - A$) behavior of lipid monolayers can be described by

$$\Delta V = 37.7\mu_{\perp}/A + \Delta V_0 \quad (\text{Eq. 5})$$

where ΔV is the potential measured in millivolts and μ_{\perp} is the dipole moment (in milliDebyes) perpendicular to the lipid-water interface and can be determined from the slope of ΔV versus $1/A$ plots (30). The intercept term, ΔV_0 , is lipid-specific and appears to arise from an epitaxial ordering of interfacial water molecules (30, 33). ΔV versus $1/A$ plots of various liquid-expanded lipids are linear from ~ 1 mN/m up to surface pressures at which the second derivative of the π - A isotherms ($d^2\pi/dA^2$) goes from positive to negative values (π_d) (33, 34). The linearity indicates a lack of significant dipole reorientation over the range of surface pressures leading up to π_d and typically encompasses 80–90% of the $\pi - A$ data for liquid-expanded films.

Monolayer compressibilities at the indicated experimental mixing ratios were obtained from $\pi - A$ data using:

$$C_s = -\frac{1}{A} \left(\frac{\partial A}{\partial \pi} \right)_T \quad (\text{Eq. 6})$$

where A is the area per molecule at the indicated surface pressure (π). To facilitate comparison with elastic moduli of area compressibility values in bilayer systems, we expressed our data as the reciprocal of C_s , originally defined as the surface compressional modulus (C_s^{-1}) by Davies and Rideal (35). High C_s^{-1} values correspond to low lateral elasticity among packed lipids forming

the monolayer. Comprehensive descriptions of the mechanoelastic properties of model membranes have been reviewed by Needham (36), Behroozi (37), and Brown and Brockman (38). Whenever possible, we used a 100 point sliding window that used every fourth point to calculate a C_S^{-1} value before advancing the window one point. Reducing the window size by 5-fold did not significantly affect the observed C_S^{-1} values. Each plot of C_S^{-1} versus average molecular area consisted of 200 C_S^{-1} values obtained at equally spaced molecular areas along the $\pi - A$ isotherms. The standard errors of our C_S^{-1} values are $\sim 2\%$. C_S^{-1} values, which use data available in the slopes of the isotherms, respond to changes in surface pressure and phase state. C_S^{-1} values are known to be especially sensitive to phosphatidylcholine acyl structure during mixing with cholesterol at high surface pressures that mimic the biomembrane environment (39–41). C_S^{-1} data complement area condensation data, which are inherently less reliable at high surface pressures because of the small changes that occur in average area.

The area-condensing effect of cholesterol on different phosphatidylcholine species was determined from plots of average molecular area versus composition (39, 41–43). Experimentally observed areas of mixtures were compared with areas calculated by summing the molecular areas of the pure components (apportioned by mole fraction in the mixture). The calculated average molecular area (A) of two component mixtures was determined at a given surface pressure (π) using the following equation:

$$A = X_1(A_1) + (1 - X_1)(A_2) \quad (\text{Eq. 7})$$

where X_1 is the mole fraction of component 1 and A_1 and A_2 are the molecular areas of pure components 1 and 2 at identical surface pressures. Negative deviations from additivity indicate area condensation and imply intermolecular accommodation and/or dehydration interactions between the lipids in the mixed films.

RESULTS

Me₄-BODIPY-8 probe synthesis

Figure 1 summarizes the syntheses of the Me₄-BODIPY-8-labeled fatty acids (XIII–XVI) and their insertion into complex lipids (XVII–XX), which have been described in detail previously (20). Briefly, for the preparation of acids XIII–XVI, the route of Burghart et al. (44) was followed, with minor modifications. Monomethyl acid chlorides, derivatives of succinic (I) adipic (II), suberic (III), and sebacic (IV) acid, were reacted with 2,4-dimethylpyrrole to obtain the corresponding dipyrromethene derivatives (V–VIII). These rather unstable intermediates were treated without isolation with boron trifluoride etherate and triethylamine, resulting in the Me₄-BODIPY-8 fatty acid methyl esters (IX–XII) in yields of 23–28% after silica gel column chromatography. Because of the well-known sensitivity of BODIPY to alkali (8), carefully controlled alkaline hydrolysis (0.1 N aqueous KOH-isopropanol, 2:5; 20°C) was needed to obtain 85–95% yields of the desired key acids, ω -(4,4-difluoro-1,3,5,7-tetramethyl-4-bora-3a,4a-diaza-s-indacene-8-yl)-propionic (XIII), -pentanoic (XIV), -heptanoic (XV), and -nonanoic (XVI) acid. It should be mentioned that acids XIII and XVI are manufactured by Invitrogen, but their high cost restricts their availability. Phosphatidylcholines, XVII (B3-PC), XVIII (B5-PC), XIX (B7-PC), and XX (B9-PC), bearing the above acids were

prepared by acylation of lysophosphatidylcholine (derived from egg yolk phosphatidylcholine) with the corresponding acid in the presence of dicyclohexylcarbodiimide (5).

Probe spectral properties in solution and in bilayers

The absorption and fluorescence spectra of probes XVII–XXII and their corresponding acids XIII–XVI in ethanol are nearly identical, sharing similar characteristics with other Me₄-BODIPY-8 derivatives (15), with absorption maximum at 498 nm (ϵ 8–10 $\times 10^4$ M⁻¹ cm⁻¹; in ethanol). The fluorescence spectra show excitation maxima at 497–498 nm and emission maxima at 506–508 nm, typical for BODIPY derivatives (15). Representative excitation and emission spectra, for phosphatidylcholine probe B7-PC in DMPC vesicles, are shown in Fig. 2A. The fluorescence spectra measured in solvents of different polarity were similar (data not shown), in agreement with previous reports indicating low environmental sensitivity for BODIPY fluorescence (9, 10). The quantum yields of the Me₄-BODIPY-8 derivatives described here were not determined absolutely, but comparative measurements of relative fluorescence intensities in ethanol of acids XIII–XVI and of known BODIPY probes [D-2190 and D-3834 products of Invitrogen; quantum yields ≥ 0.9 (13)] revealed no noticeable differences.

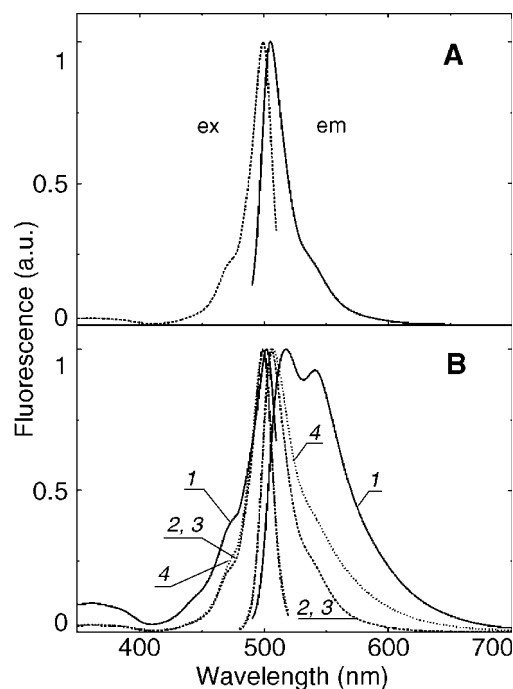


Fig. 2. Normalized excitation ($\lambda_{em} = 510$ nm) and emission ($\lambda_{ex} = 480$ nm) spectra of Me₄-BODIPY-8 probes. A: B7-PC in 1,2-dimyristoyl-*sn*-glycero-3-phosphocholine (DMPC) vesicles (0.4 mg/ml) suspended in PBS, probe-lipid molar ratio of 1:1,000, at 37°C. B: Peak 1, ester XI, 5% solution (w/v) in chloroform, at 20°C (for other experimental details, see Materials and Methods). Peaks 2–4, B7-PC in POPC vesicles suspended in PBS at 20°C: 0.1 mol% probe, total lipid 0.8 mg/ml (peak 2); 5 mol% probe, total lipid 0.02 mg/ml (peak 3); and 10 mol% probe, total lipid 0.008 mg/ml (peak 4). a.u., arbitrary units.

To determine whether Me₄-BODIPY-8 can form fluorescent dimers, a characteristic of Me₂-BODIPY-3 derivatives (18, 19), we measured spectra of Me₄-BODIPY-8 probe at high solution concentrations. This was done first using methyl ester **XI**, because of its good solubility in organic solvents. Excitation and emission spectra of a 5% (~0.13 M) solution in chloroform are shown in Fig. 2B. To reduce the side effects of strong absorption at high concentration (i.e., inner filter effects), measurements were carried out in thin glass capillaries to provide short light paths for both excitation and emission (45). Under these conditions, the excitation spectrum showed a red-shifted wavelength maximum (~4 nm) compared with dilute fluorophore in DMPC (Fig. 2A). In the emission spectrum, dramatic changes were evident at high Me₄-BODIPY-8 solution concentrations. Apart from a red shift of the wavelength maximum from 506–508 to 518 nm, a new peak appeared at ~540 nm (Fig. 2B, peak 1), which seemed to result from the high probe concentrations in the capillaries, in which calculated peak absorbance can exceed 500 even at path lengths as short as 0.05 cm. However, there was no evidence of the longer wavelength emission peak (620–630 nm region) that has been associated previously with emission by BODIPY dimers (18, 19).

The effects of high Me₄-BODIPY-8 concentrations on fluorescence spectra of POPC vesicles containing 0.1, 5, and 10 mol% B7-PC probe were evaluated using total lipid concentrations that yielded nearly equal optical absorbances of ~0.08 in the mixtures (Fig. 2B, peaks 2–4). The spectra registered at 0.001 (peak 2) and 0.05 (peak 3) probe mole fractions coincided with each other and with the spectrum of the 0.001 B7-PC mole fraction in DMPC (Fig. 2A). Although negligible change was observed in the excitation spectrum at 10 mol% B7-PC probe, broadening of the emission spectrum to the red side began to show (Fig. 2B, peak 4). Again, no sign of a peak in the 620–630 nm region was visible.

Probe lateral packing and spectral properties in monolayers

To investigate the lateral packing features of B7-PC in monolayers, the surface pressure versus average molecular area behavior was measured using an automated Langmuir-type film balance capable of collecting fluorescence emission spectra during monolayer compression (see Materials and Methods). **Figure 3A** shows the force-area isotherms of B7-PC (Me₄-BODIPY-8) compared with several phosphatidylcholines containing acyl chains with different *cis*-unsaturation and commercial BODIPY-PC (PB-PC) containing Me₂-BODIPY-3 (Fig. 1). The attachment of Me₄-BODIPY-8 fluorophore to phosphatidylcholine resulted in its molecular cross-sectional area being slightly larger than that of the PB-PC fluorophore or naturally occurring, highly unsaturated acyl chains. The cross-sectional molecular area of phosphatidylcholine containing Me₄-BODIPY-8 (B7-PC) at 30 mN/m, a surface pressure mimicking biomembrane conditions, was consistent with fluid-like lateral packing of the hydrocarbon region, in which the phospho-

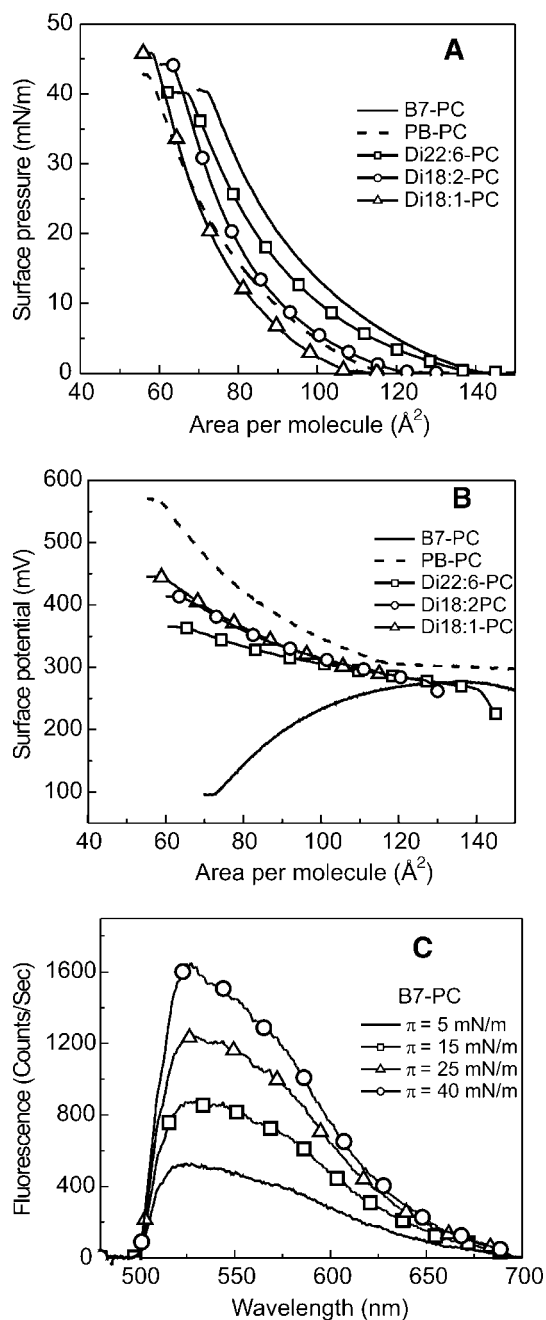


Fig. 3. Monolayer behavior of pure B7-PC. A: Surface pressure versus average cross-sectional molecular area isotherms (24°C) of B7-PC (line lacking symbols), of phosphatidylcholines (PCs) containing acyl chains with different *cis*-unsaturation (dioleoyl = triangles; dilinoleoyl = circles; didocosahexenoyl = squares), and of PB-PC (dashed line). B: Surface potential versus average cross-sectional area isotherms of B7-PC and of the same phosphatidylcholines as in A. C: Fluorescence emission spectra of B7-PC monolayers at surface pressures of 5 mN/m (line lacking symbols), 15 mN/m (line marked by squares), 25 mN/m (line marked by triangles), and 40 mN/m (line marked by circles). Additional experimental details are described in Materials and Methods.

tidylcholine acyl chain containing the Me₄-BODIPY-8 embeds in the hydrophobic interior of the lipid monolayer. Also evident under membrane-like packing conditions was the slightly lower C_s^{-1} , indicating higher lateral

packing elasticity in the B9-PC films compared with phosphatidylcholines with unsaturated acyl chains (Table 1).

To determine how the molecular dipole properties of phosphatidylcholine are affected by Me₄BODIPY-8, the dipole potential of B7-PC was measured as a function of molecular cross-sectional area and compared with data obtained for PB-PC and for different naturally occurring phosphatidylcholine species. Figure 3B shows that, as the B7-PC monolayer is compressed, its dipole potential decreases, in marked contrast to the continuously increasing potential that is typical for unsaturated phosphatidylcholines and for PB-PC. At collapse, the dipole potential is 104 mV, a value ~350 and 450 mV lower than for unsaturated phosphatidylcholines and for PB-PC, respectively. Table 1 summarizes the values of μ_{\perp} and ΔV_0 , obtained from plots of the dipole potential versus inverse cross-sectional molecular area ($V - A^{-1}$). ΔV_0 values for B7-PC were 551 mV, compared with 24 mV for PB-PC (26) and 110–140 mV for the fluid nonfluorescent phosphatidylcholines lacking docosahexenoyl acyl chains (30, 33, 34). However, the dipole moment, μ_{\perp} , of B7-PC was found to be -850 milliDebyes, compared with 874 milliDebyes for PB-PC (26) and 480–550 milliDebyes for phosphatidylcholines lacking docosahexenoyl acyl chains (30, 33, 34).

The fluorescence emission response of pure B7-PC monolayers during compression is shown in Fig. 3C. The emission spectra show a peak ($S_0 \rightarrow S_1$) in the vicinity of 520 nm with a shoulder at ~540 nm that is characteristic of BODIPY fluorophores (10) but no evidence of the 620–

630 nm “signature” emission peak characteristic of Me₂BODIPY-3 dimers (32). Even so, there was considerable broadening of the B7-PC emission spectrum, caused by an apparent increase in intensity near 570 nm as well as an overall increase in emission intensity with increasing surface pressure (Fig. 3C).

Mixing of B7-PC with POPC had little effect on the force-area isotherm of POPC at low B7-PC mole fractions (e.g., 0.01) (Fig. 4A). The small effect of B7-PC on the POPC isotherm, at probe mole fractions of 0.1 and 0.2, suggested a slight ordering effect on POPC by the higher probe concentrations. Consistent with this conclusion was the slight negative deviation from the calculated ideal additivity in average molecular area versus composition plots (data not shown). Figure 4B–E show the fluorescence emission response for the various B7-PC/POPC mixtures measured at different surface pressures. The broadness of the peaks increases at elevated B7-PC mole fractions and surface pressures. Concurrent with the changes in emission broadness are incremental shifts (515–528 nm range) in the wavelength maximum associated with monomer emission ($S_0 \rightarrow S_1$). The magnitude of the shift in wavelength maximum was found to depend upon the surface concentration of the B7-PC probe (Fig. 4F).

To evaluate the effect of different mole fractions of B7-PC in POPC mixtures containing cholesterol, force-area isotherms were measured while simultaneously collecting fluorescence spectra of monolayers containing 0.33 mol fraction of cholesterol. The isotherms shown in Fig. 5A indicate that the B7-PC probe does have a small effect on the POPC/cholesterol (2:1) isotherm, especially at relatively high probe mole fractions (e.g., 0.1). To further assess the nature of this effect, both the area condensation and change in C_S^{-1} induced by cholesterol were evaluated in the presence of different B7-PC mole fractions. Figure 5B shows the well-established area condensation resulting from the presence of cholesterol in the phosphatidylcholine monolayers. POPC exists in a fluid, liquid-expanded phase state at both low and high surface pressures (5 and 30 mN/m). Because the cross-sectional molecular area of pure cholesterol is very similar at low and high surface pressure (e.g., 37.6 Å/molecule at 5 mN/m and 36.8 Å/molecule at 30 mN/m) and smaller than that of phosphatidylcholine, increasing the cholesterol mole fraction reduces the average molecular area in the mixed monolayers. However, the experimentally observed areas (left symbols) in the mixtures are smaller than the predicted areas, calculated from the additive behavior of each pure lipid (stars). The larger than expected decrease in the average molecular area indicates a chain-ordering effect of cholesterol on phosphatidylcholine. This so-called “condensing effect” by cholesterol is clearly evident during mixing with fluid, liquid-expanded phosphatidylcholines (e.g., POPC) (39, 42) that contain 0.01, 0.1, or 0.2 mol fraction B7-PC (Fig. 5B). A manifestation of the cholesterol-induced ordering of the phosphatidylcholine chains is decreased lateral elasticity (i.e., increased C_S^{-1}) in the POPC/sterol mixture. The presence of B7-PC at mole fractions up to 0.1 was found to

TABLE 1. Monolayer properties of phosphatidylcholines containing Me₄BODIPY-8 fluorophore, Me₂BODIPY-3 fluorophore, or unsaturated acyl chains

Lipids	Area	C_S^{-1}	μ_{\perp}	ΔV
	($\pi = 30$ mN/m)	($\pi = 30$ mN/m)		
	Å ²	mN/m	mV	
Me ₄ BODIPY-8 phosphatidylcholine	80	96	-850	551
1-Palmitoyl-2-Me ₂ -BODIPY-3-pentanoyl- <i>sn</i> -glycero-3-phosphocholine	65.8	88	874	24
DOPC	66.3	116	530	113
DLPC	70.4	116	480	134
DAPC	71.7	106	515	117
DDPC	75.1	96	310	188
POPC	62.9	124	515	107
PLPC	65.8	122	502	134
PAPC	67.4	115	553	112
PDPC	70.2	107	461	155

Me₄BODIPY-8, 4,4-difluoro-1,3,5,7-tetramethyl-4-bora-3a,4a-diaza-s-indacene-8-yl. The acronyms for 1,2-diacyl-*sn*-glycero-3-phosphocholines (PCs) are as follows: DOPC, 1,2-dioleoyl-PC; DLPC, 1,2-dilinoleoyl-PC; DAPC, 1,2-diarachidonoyl-PC; DDPC, 1,2-didocosahexenoyl-PC; POPC, 1-palmitoyl-2-oleoyl-PC; PLPC, 1-palmitoyl-2-linoleoyl-PC; PAPC, 1-palmitoyl-2-arachidonoyl-PC; PDPC, 1-palmitoyl-2-docosahexenoyl-PC. An improved fit resulted for the ΔV versus $1/A$ plot of Me₄BODIPY-8 phosphatidylcholine when fitting from 10 mN/m (instead of 1 mN/m) to collapse, as described in Materials and Methods. The resulting μ_{\perp} and ΔV values were -975 and 605 mV, respectively. C_S^{-1} , μ_{\perp} , and ΔV values for the various phosphatidylcholine species and for Me₂BODIPY-3 phosphatidylcholine are taken from Refs. 33, 24, and 26, respectively.

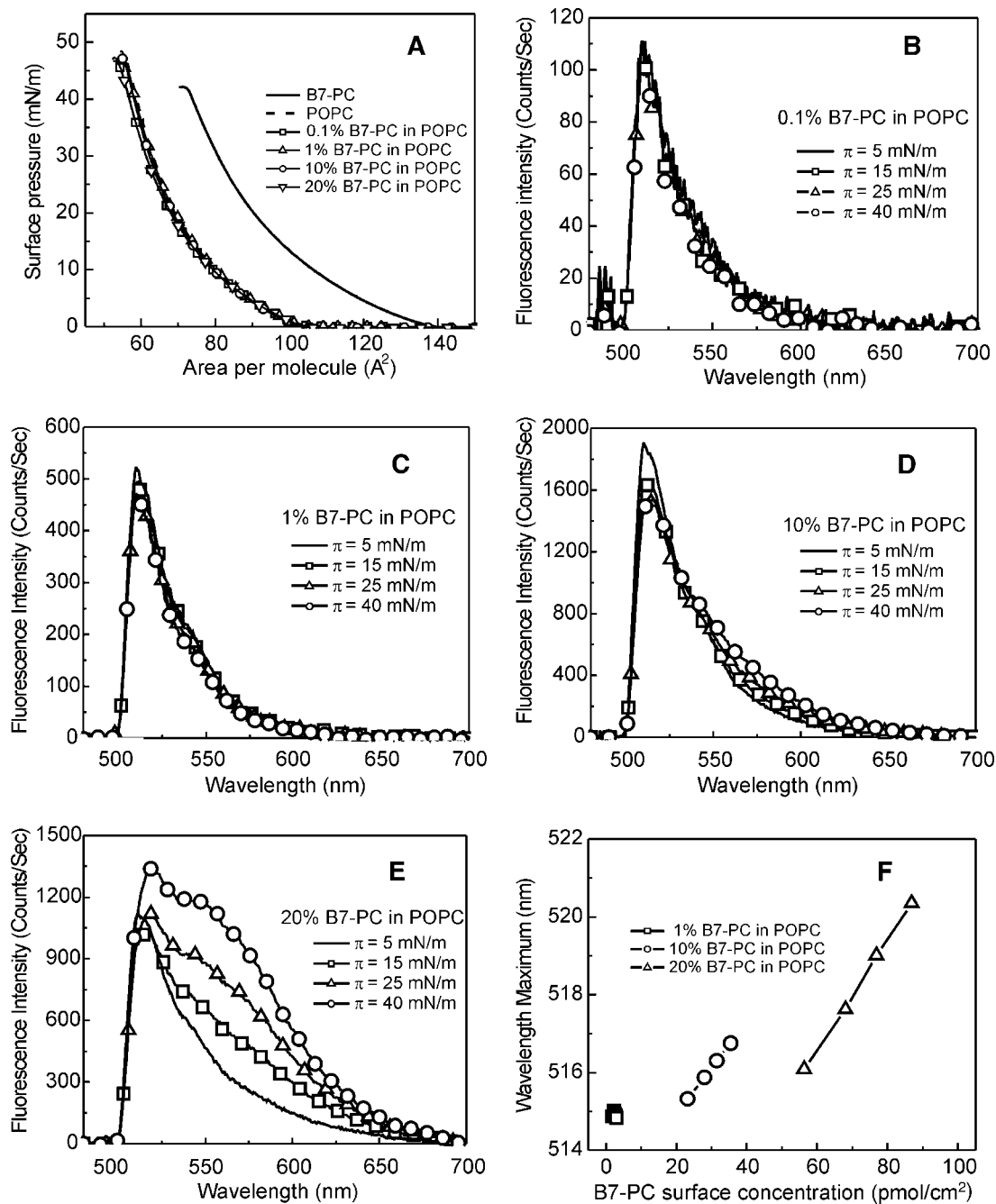


Fig. 4. Monolayer behavior of B7-PC mixed with POPC. A: Surface pressure versus average cross-sectional molecular area isotherms (24°C) of B7-PC (line lacking symbols) and B7-PC mixed at mole fractions of 0.001 (line marked by squares), 0.01 (line marked by triangles), 0.1 (line marked by circles), and 0.2 (line marked by inverted triangles) with POPC. B–E: Fluorescence emission spectra of B7-PC mixed at mole fractions of 0.001 (B), 0.01 (C), 0.1 (D), and 0.2 (E) with POPC at surface pressures of 5 mN/m (lines lacking symbols), 15 mN/m (lines marked by squares), 25 mN/m (lines marked by triangles), and 40 mN/m (lines marked by circles). F: Emission wavelength maximum as a function of B7-PC surface concentration. B7-PC mole fractions of 0.01 (squares), 0.1 (circles), and 0.2 (triangles) mixed with POPC are shown at surface pressures of 5, 15, 25, and 40 mN/m, with the highest surface pressure corresponding to the highest wavelength maximum.

have no significant effect on the C_s^{-1} values of the POPC/cholesterol (2:1) mixed monolayers (data not shown).

The emission spectra for POPC/cholesterol (2:1) monolayers containing different mole fractions of B7-PC are shown in **Fig. 6A–C**. The data indicate that the presence of cholesterol enhances the spectral broadening of

the B7-PC probe compared with POPC monolayers lacking sterol, as is evident by comparing films containing 0.1 mol fraction of B7-PC (Figs. 4D, 6C). Accompanying the enhanced spectral broadening is an enhanced red shift in the emission wavelength maximum (Fig. 6D), reflecting the increase in B7-PC surface concentration that results

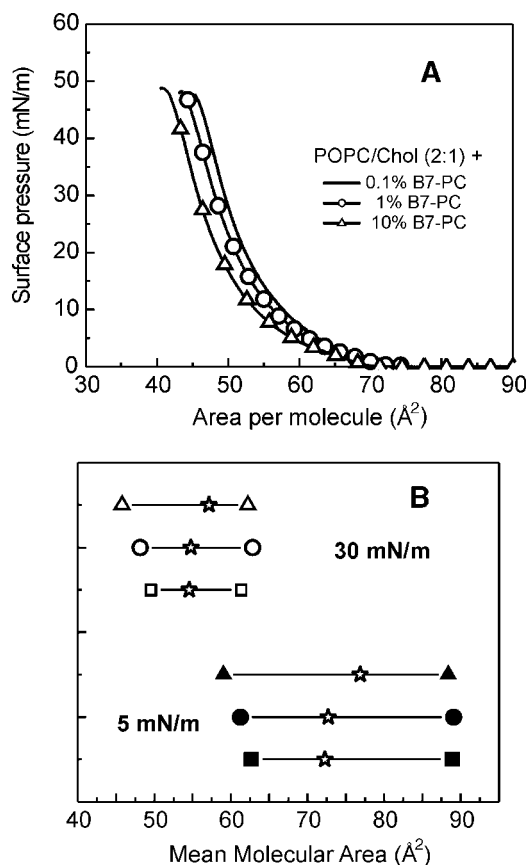


Fig. 5. Monolayer behavior of B7-PC mixed with POPC/cholesterol (Chol). A: Surface pressure versus average cross-sectional molecular area isotherms of B7-PC mixed at mole fractions of 0.001 (line lacking symbols), 0.01 (line marked by circles), and 0.1 (line marked by triangles) with POPC/cholesterol (2:1) at 24°C. B: Cholesterol-induced molecular area condensation in POPC/cholesterol (2:1) mixed monolayers in the presence of various B7-PC mole fractions. B7-PC mole fractions are 0.001 (squares), 0.01 (circles), and 0.1 (triangles). Upper grouping of open symbols = 30 mN/m; lower grouping of closed symbols = 5 mN/m. All right-hand symbols = molecular area in the absence of cholesterol; all left-hand symbols = average molecular area in the presence of cholesterol. Stars represent the calculated additivity predicted from the areas of all three lipid components in pure form.

from the cholesterol-induced phosphatidylcholine increase in chain ordering and reduction in cross-sectional area.

Probe location in bilayers by iodide quenching

To determine the depth of fluorophore immersion in the bilayer, Me₄-BODIPY-8 accessibility was investigated by iodide quenching using a phosphatidylcholine set (B3-PC, B5-PC, B7-PC, and B9-PC) in which increasingly longer methylene linker chains separated the probe and the carboxyl ester group. In quenching experiments with KI and NaI (9, 46), precautions were taken to avoid artifacts that cause changes in signal intensity by means other than quenching (see Materials and Methods). Artifactual contributions to emission intensity can be caused by simple dilution effects as well as by light scattering originating from the vesicles. Typically, correction for such effects is

achieved by performing control measurements on vesicles containing no fluorophore and subtracting this background signal (47). However, this kind of correction takes into account only the light-scattering change of the excited light without allowing for scattering of emitted light and does not adequately account for the fact that the light-scattering signal originating from liposomes is a complex process, which depends not only on vesicle size and shape but also on the refraction index changes at the interfacial boundary (26, 27). To avoid the latter problems, we corrected in the following way. Control measurements were performed with vesicles containing BODIPY probe, using a nonquenching NaCl solution at concentrations and aliquot sizes identical to those of quenching NaI solution (see Materials and Methods). Both the NaCl and NaI stock solutions have, at the same concentrations, virtually the same refractive indexes (data not shown), providing sufficient correction for scattering effects produced by changes of light refraction at bilayer/solution interfaces. It should be noted that a similar approach for correction of the inner filter effect in suspensions of fluorescent particles was applied previously by Subbarao and MacDonald (48).

Figure 7 shows Stern-Volmer plots obtained during quenching of the probes in DMPC vesicles at 17°C (Fig. 7A) and 37°C (Fig. 7B) as well as in DMPC/cholesterol (7:3) vesicles at 37°C (Fig. 7C). The latter composition was chosen because DMPC/cholesterol mixtures with a sterol content of ≥25–30 mol% form liquid-ordered phase (49) and the phase homogeneity can be expected to simplify the interpretation of results. Similar quenching analyses also were performed with the probes in POPC vesicles at 17°C (Fig. 8A) and 37°C (Fig. 8B). The quenching in the POPC vesicles at 37°C was compared with data obtained using AV12-PC (Fig. 8B), a fluorophore known to embed deeply in the bilayer (5). K_{sv} values for the data in Figs. 7 and 8A, B are listed in Table 2.

As another control in which the Me₄-BODIPY-8 fluorophore undoubtedly exists as two populations, one accessible and one inaccessible to the iodide quenching, a system was prepared in which POPC vesicles were doped with phosphatidylcholine probe B3-PC together with an equimolar quantity of the corresponding moderately water-soluble acid XIII (Fig. 8C, upper trace). Quenching of B3-PC alone in vesicles is also shown (Fig. 8C, lower trace). The data reveal that Me₄-BODIPY-8 probes are quenched by iodide in bilayers, although much less efficiently than in water solution (9). Stern-Volmer plots for quenching of the single probe-labeled vesicles (Figs. 7A–C and 8A, B) are linear ($r \geq 0.98$). The lack of curvature toward the x axis is consistent with a single fluorophore population (50). It is reasonable to expect this single population of fluorophores to be embedded in the bilayer at the maximal depth allowed by the acyl bearer.

In all cases, B3-PC, which bears fluorophore at the shortest distance from the polar head, is quenched most efficiently, with K_{sv} being largest compared with the other probes (Table 2). This finding is consistent with a shallow position in bilayer by the B3-PC probe fluorophore. At the

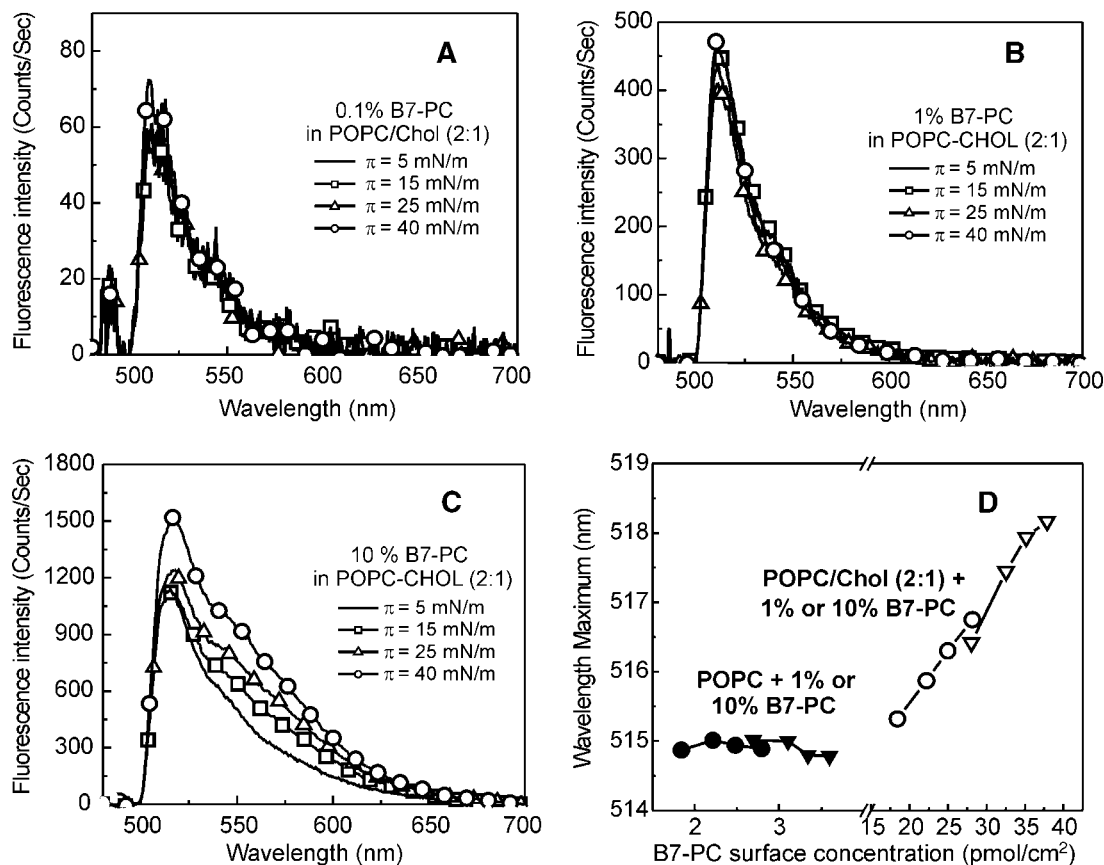


Fig. 6. Fluorescence emission response of POPC/cholesterol (Chol) mixed monolayers containing B7-PC. A–C: Fluorescence emission spectra of POPC/cholesterol (2:1) monolayers containing B7-PC mixed at mole fractions of 0.001 (A), 0.01 (B), and 0.1 (C) at surface pressures of 5 mN/m (lines lacking symbols), 15 mN/m (lines marked by squares), 25 mN/m (lines marked by triangles), and 40 mN/m (lines marked by circles). D: Emission wavelength maximum as a function of B7-PC surface concentration in POPC and POPC/cholesterol (2:1) monolayers. B7-PC mole fractions of 0.01 (circles) and 0.1 (triangles) mixed with either POPC (closed symbols) or POPC/cholesterol (2:1) (open symbols) are shown at surface pressures of 5, 15, 25, and 40 mN/m, with the highest surface pressure corresponding to the highest wavelength maximum.

same time, the Me₄-BODIPY-8 fluorophore of B3-PC in vesicles is not freely accessible to water molecules. This conclusion follows from the fact that, in vesicle preparations labeled with B3-PC and acid **XIII** in which the latter is located mainly in water phase (spectrophotometric assessment; data not shown), the Me₄-BODIPY-8 fluorophore is quenched much more efficiently (Fig. 8C, upper trace), with initial apparent $K_{sv} = 10.3$. In this case, the Stern-Volmer plot clearly bends toward the x axis compared with quenching of phosphatidylcholine B3-PC (Fig. 8C, lower trace), confirming the presence of two fluorophore populations in this system.

The other probes tested, B5-, B7-, and B9-PC, are quenched less efficiently by iodide than B3-PC, consistent with the I⁻ concentration diminishing gradually toward the bilayer center and resulting in decreased quenching efficiency and K_{sv} values, in accordance with the fluorophore distance from the polar head. This finding holds true for the quenching in DMPC vesicles at 17°C and in POPC vesicles at 37°C (Figs. 7A, 8B). Table 2 shows that their K_{sv} values differ by only 10–15%. In the DMPC bilayer at 17°C [i.e., below the phase transition temper-

ature (T_m) of 24°C], the K_{sv} values are lowest. In contrast, they are highest in POPC vesicles at 37°C, a temperature well above the T_m of -2°C (Table 2). In liquid-crystalline bilayers at temperatures not far from T_m [DMPC at 37°C (Fig. 7B), POPC at 17°C (Fig. 8A)], deviations from such order occurred, reflecting the complicated profile of the iodide distribution.

When the DMPC vesicles contained cholesterol (0.3 mol fraction), the I⁻ quenching responses of B5-, B7-, and B9-PC were similar to each other, within experimental error (Fig. 7C). The K_{sv} values (Table 2) were intermediate between those observed for the same probes in pure DMPC at 17°C (gel phase) and 37°C (liquid-crystalline phase), perhaps reflecting the liquid-ordered nature of the system.

Compared with all Me₄-BODIPY-8 probes, iodide quenching of anthrylvinyl probe AV12-PC is least efficient (Fig. 8B), consistent with a deep localization of anthrylvinyl near the bilayer center. The linear nature of the Stern-Volmer quenching plot for this anthrylvinyl probe ($r = 0.91$) provides evidence for a single probe population. These findings are not surprising given the length of the spacer hydrocarbon (12 carbon atoms) and the apolar

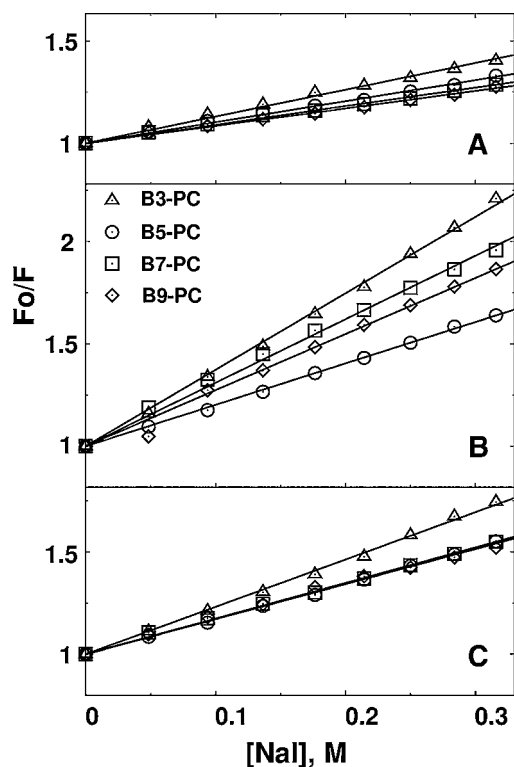


Fig. 7. Stern-Volmer quenching plots of probes B3-PC, B5-PC, B7-PC, and B9-PC in DMPC vesicles at 17°C (A), in DMPC vesicles at 37°C (B), and in DMPC/cholesterol (7:3) vesicles at 37°C (C). Lipid concentration was 0.4 mg/ml; probe-lipid molar ratio was 1:1,000.

nature of the anthrylvinyl fluorophore in AV12-PC. The middle-of-the-bilayer localization for the anthrylvinyl fluorophore in AV12-PC revealed by the quenching data is consistent with earlier $^1\text{H-NMR}$ data (5).

Fluorophore depth in the bilayer determined by parallax analysis

To confirm the bilayer location of the $\text{Me}_4\text{-BODIPY-8}$ fluorophore and more precisely estimate the fluorophore depth in the bilayer, we used the parallax quenching approach, involving fluorescence quenching by two quenchers with different, fixed positions in the bilayer (17, 28). Large unilamellar POPC vesicles, doped with B3-, B5-, B7-, or B9-PC probe, were quenched with phosphatidylcholines bearing either 7-iodoheptanoyl (I7-PC) or 11-iodoundecanoyl (I11-PC) *sn*-2 acyl chains (Fig. 1). Use of the iodine atom as a quencher minimally altered the polarity of the aliphatic chain, as was evident by the nearly identical thin-layer chromatographic mobilities of 11-iodoundecanoic acid and dodecanoic acid. Thus, the behavior of 7-iodoheptanoyl and 11-iodoundecanoyl chains in bilayers is similar to that of bromoacyls (50), and the iodine atom can be expected to locate at the maximal allowed depth, with deviations induced by thermal mobility of chains. In our case, the quencher concentration was limited to 5 mol% to minimize the distortion of the bilayer and avoid separation of the quencher into a separate phase.

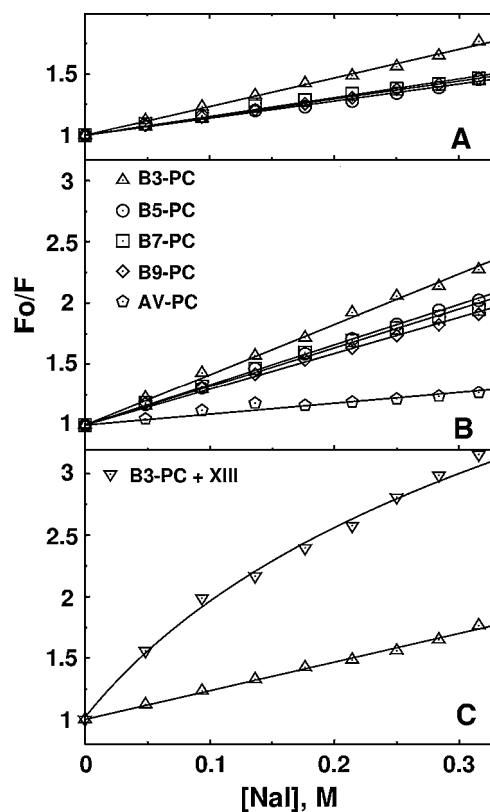


Fig. 8. Stern-Volmer quenching plots of probes B3-PC, B5-PC, B7-PC, and B9-PC in POPC vesicles at 17°C (A), of probes B3-PC, B5-PC, B7-PC, B9-PC, and AV12-PC in POPC vesicles at 37°C (B), and of probe B3-PC (lower trace) and probes B3-PC + XIII in equimolar concentrations (upper trace) in POPC vesicles at 37°C (C). Lipid concentration was 0.4 mg/ml; probe mole fraction was 0.001 (A, B, and C, lower trace) or 0.002 (C, upper trace).

Based on the assumption that the liquid-crystalline POPC bilayer is 35 Å thick at 20°C, the distance of the iodine atom from the bilayer center is ~ 8.8 Å for I7-PC and ~ 5.8 Å for I11-PC (see Materials and Methods).

TABLE 2. Stern-Volmer quenching constant values for iodide quenching $\text{Me}_4\text{-BODIPY-8}$ and anthrylvinyl phosphatidylcholine probes in vesicles

Probe	Vesicle Composition and Temperature				
	DMPC, 17°C	DMPC, 37°C	DMPC/Cholesterol (7:3), 37°C	POPC, 17°C	POPC, 37°C
B3-PC	1.31	3.73	2.31	2.33	4.12
B5-PC	1.03	2.02	1.72	1.39	3.30
B7-PC	0.91	3.10	1.74	1.53	3.17
B9-PC	0.85	2.74	1.71	1.47	2.94
1-Acyl-2-[12-(9-anthryl)-11E-dodecenoyl]- <i>sn</i> -glycero-3-phosphocholine	—	—	—	—	0.89

B3-, B5-, B7-, or B9-PC, phosphatidylcholine bearing at the *sn*-2 position $\omega\text{-Me}_4\text{-BODIPY-8-C}_3\text{-, -C}_5\text{-, -C}_7\text{-, or -C}_9\text{-fatty acid}$, respectively; DMPC, 1,2-dimyristoyl-*sn*-glycero-3-phosphocholine. The values were derived from the plots shown in Figs. 2, 3 as described in Materials and Methods.

Calculation of the Me₄-BODIPY-8 fluorophore location from the bilayer center was performed for all four probes by parallax analysis (Table 3). The distances from the bilayer center to the fluorophore increased in the order B9-PC < B7-PC < B5-PC < B3-PC (Table 3), in agreement with the pattern obtained by soluble iodide quenching (Table 2).

DISCUSSION

The spectral parameters of the Me₄-BODIPY-8 fluorophore (absorption and fluorescence maxima, quantum yield, etc.) strongly resemble those of other methylated members of the BODIPY family (15). However, one noteworthy feature of Me₄-BODIPY-8 distinguishing it from analogs containing the Me₂-BODIPY-3 fluorophore is the lack of an emission peak near 630 nm. This peak, which is clearly observed at high Me₂-BODIPY-3 concentrations, was originally proposed to be caused by the formation of "excimers" (i.e., excited state dimers) (9, 18, 32), based on apparent similarities with the emission behavior of pyrene (51–53). However, comprehensive photophysical analyses by Johansson and colleagues (19, 54) have shown that the so-called excimer peak actually results from the emission of ground-state BODIPY dimers, denoted D_{II}, in which the BODIPY rings are coplanar with their S₀→S₁ transition dipoles aligned at ~55°, resulting in absorption near 570 nm and emission near 630 nm. Energy transfer to the ground-state D_{II} dimers from excited-state monomers is typically responsible for the D_{II} emission peak observed near 630 nm. A second type of ground-state dimer, denoted D_I, characterized by a sandwich-like stacking of the BODIPY rings resulting in parallel alignment of the transition dipoles and absorption near 477 nm, produced no fluorescence emission after excitation (19, 54).

Even though an emission peak near 630 nm is not observed at high concentrations for Me₄-BODIPY-8 phosphatidylcholine derivatives, substantial broadening of the emission spectrum does occur because of increased fluorescence near 570 nm relative to the 510–520 nm region. The persistence of emission broadening when the total absorbance is low (<0.1) in the bilayers (Fig. 2B) and monolayers (Figs. 2, 3, 5) suggests the involvement of

excimer or dimer fluorescence rather than an inner filter effect. However, unequivocal determination among these possibilities will require the application of comprehensive photophysical approaches. Regardless, because the changes in emission broadness and wavelength maximum depend upon the surface concentration of B7-PC, the Me₄-BODIPY-8 can be expected to be a useful probe for detecting lateral heterogeneity when attached to other lipids (i.e., sphingolipids).

What is clear from the monolayer analyses of Me₄-BODIPY-8 phosphatidylcholine is that the probe mimics the behavior of fluid-phase phosphatidylcholines with unsaturated acyl chains reasonably well and does not perturb lipid packing so long as the fluorophore concentration is kept low (e.g., ≥1 mol%). At higher mole fractions (e.g., 10 or 20 mol%), the probe begins to exert its own influence on the system rather than serving as an "impartial" reporter. Such findings are not surprising and are commonly observed for virtually all probe molecules.

Compared with lipid probes carrying the Me₂-BODIPY-3 fluorophore, the Me₄-BODIPY-8 fluorophore shows an enhanced tendency for localizing within the apolar region of the bilayer, with the penetration depth dictated by the length of the connecting hydrocarbon chain. This conclusion is supported by the iodide quenching analyses of phosphatidylcholines with different length connecting chains to the Me₄-BODIPY-8 fluorophore. Iodide is known to be an effective quencher of BODIPY fluorescence (9), and this small, modestly hydrated anion does not change lipid bilayers when used in concentrations up to 0.5 M (46). It is well known that iodide anions can penetrate into phospholipid bilayers (50), although the details of the transbilayer distribution of iodide remain unclear. Among other quenchers, nitroxide-labeled lipids have been used to determine the immersion depth of different BODIPY probes in bilayers (17). However, we did not use doxyl quenchers because of reported distortions of membrane structure (55, 56) that can occur at doxyl concentrations needed for efficient quenching [~15 mol% doxyl (17)]. Also, doxyl labels attached to lipid hydrocarbon chains are broadly distributed in the membrane (57), complicating their use for precise determination of the fluorophore depth. It also should be noted that, among free quenchers tested for this study, iodide was the most effective. Quenchers such as free cesium cation and acrylamide did not quench Me₄-BODIPY-8 fluorescence, either in bilayers or in homogeneous water solution (data not shown).

As for the iodide distribution across the bilayer, this issue has been considered by several research groups and the general consensus is that a concentration gradient forms during equilibration with iodide. Cranney et al. (58) noted that the quenching efficiency of diphenylhexatriene and its derivatives by iodide correlated with the extent of the fluorophore immersion and considered strong quenching as evidence of shallow fluorophore location. Such findings imply a transbilayer iodide gradient that is low near the bilayer center. Although such a conclusion was not explicitly stated by the authors, Langner and Hui (59) interpreted these data as evidence

TABLE 3. Quenching by iodolabeled phosphatidylcholines and fluorophore depth of Me₄-BODIPY-8 probes in the POPC bilayer

Probe	F ₁	F ₂	z _{CF} Found	z _{CF} Calculated
				Å
B3-PC	0.77 ± 0.00	0.93 ± 0.00	14.1 ± 3.7	11.3 ± 2.1
B5-PC	0.83 ± 0.01	0.92 ± 0.01	11.6 ± 4.0	9.6 ± 2.3
B7-PC	0.84 ± 0.03	0.91 ± 0.01	10.6 ± 3.9	7.9 ± 2.6
B9-PC	0.92 ± 0.03	0.93 ± 0.02	7.9 ± 2.6	6.6 ± 2.8

F₁ and F₂, relative fluorescence intensities (F/F₀) of the probes in the presence of shallow (phosphatidylcholine bearing 7-iodoheptanoic acid at the sn-2 position) and deeper (phosphatidylcholine bearing 11-iodoundecanoic acid at the sn-2 position) quencher, respectively; z_{CF}, fluorophore distance from the bilayer center.

of an iodide concentration gradient existing across the bilayer. Barenholz and coauthors (60) investigated the iodide quenching of pyrenyl-labeled lipids in bilayers using fluorophore embedded at different depths. They concluded that I^- concentration is somewhat lower in the internal bilayer regions, where the aromatic moieties of 10-(1-pyrenyl)decanoate and 16-(1-pyrenyl)hexadecanoate are located, relative to the fluorophore, 5-(1-pyrenyl)valerate.


Based on these previous findings, it is reasonable to assume that an iodide gradient does exist across the bilayer and that it is not necessarily linear. The situation for iodide can be considered analogous to that of water, which forms a nonlinear gradient across the bilayer with a profile that depends strongly on membrane composition and structure (61). Iodide, being a polar hydrated anion, can be expected to locate in the polar region of the bilayer predominantly together with water entities. However, iodide quenching, as with any bimolecular process, is sensitive to medium fluidity, which increases toward the center in the majority of bilayers (62), together with increased disorder (63). Thus, the higher efficiency of iodide quenching in the egg yolk phosphatidylcholine vesicles of 16-(1-pyrenyl)hexadecanoate fluorophore compared with the shallower immersed fluorophore of 10-(1-pyrenyl)decanoate (60) could reflect a contribution of the increased fluidity near the bilayer center.

Consideration of the preceding information together with our quenching data led us to conclude that the Me₄-BODIPY-8 fluorophore attached to phosphatidylcholine probes embed in the bilayer to the limit allowed by full extension of the acyl chain. In DMPC vesicles at 17°C, Stern-Volmer plots for all Me₄-BODIPY-8 probes demonstrate the lowest quenching efficiency (Fig. 7A), which is expected for a gel-state bilayer with relatively low water permeability (64), which, in turn, also reflects the permeability for iodide anions. In POPC vesicles consisting of fluid bilayers at 17°C, the water permeability is higher (64), providing increased iodide quenching efficiency (Fig. 8A, Table 2), although absolute correlation between the K_{sv} value and the expected fluorophore position in the bilayer is not observed in this case. In DMPC vesicles at 37°C (greater than T_m), the quenching efficiency increases for all probes (Fig. 7B, Table 2), also with deviations from the assumed order: the B5-PC fluorophore is quenched somewhat less efficiently than B7-PC and B9-PC. These discrepancies may result from uneven distribution of iodide within the bilayer at temperatures not far from the T_m . Although the existence of a decreasing I^- gradient toward the bilayer center seems reasonable (see above), the character of its fluctuations in particular cases remains unknown. We hypothesize that the apparent discrepancies can be explained by the opposing influences of the I^- concentration gradient and the local bilayer disorder. Although the concentration of iodide ions diminishes toward the bilayer center, the secondary effect of increased quenching rate and efficiency in the more disordered medium at the bilayer center (63) may partially override the lower local I^- concentration.

It is also noteworthy that iodide quenching efficiency in the DMPC/cholesterol vesicles decreases in comparison with that in DMPC vesicles (Fig. 7B, C), in accordance with decreased water permeability (64, 65). Apart of the shallow labeled B3-PC, all other probes are quenched with nearly equal efficiencies (Table 2). Although cholesterol condenses fluid-phase DMPC (39), thus decreasing iodide quenching efficiencies and K_{sv} value (Fig. 7B, C), the Stern-Volmer plots remain straight, confirming a single-population distribution of Me₄-BODIPY-8 fluorophore in membrane and showing that the cholesterol-induced condensation does not expel fluorophore from the bilayer interior and create dual fluorophore populations.

Verification of the Me₄-BODIPY-8 fluorophore position in the bilayer was also achieved from quenching data using parallax analysis (17, 28). However, instead of using doxyl-labeled lipids as quenchers, we used iodolabeled phosphatidylcholines, I7-PC and I11-PC, for this purpose. We also intended to use another iodolabeled phosphatidylcholine, I3-PC, but were unsuccessful because of the high instability of the 3-propanoyl iodoacid. Our strategy of using iodoacids or their derivatives as fluorescence quenchers was based on consideration of the fact that iodide anion is generally a more effective quencher than bromide (50). Indeed, for indole quenching in water, quenching by iodide proceeds with a rate constant ~ 30 times higher than that of bromide (66). In our hands, 5 mol% I7-PC or I11-PC in the POPC bilayer gave 7–24% quenching of the Me₄-BODIPY-8 emission in POPC vesicles, enabling the determination of the fluorophore positions within the bilayer with reasonable accuracy (Table 3). As expected, the B9-PC fluorophore was positioned closest to the bilayer center, and B3-PC was positioned nearest to the more polar interfacial zone. Although the fluorophore positions of the B7-PC and B5-PC probes are rather close to one another, this proximity and other small discrepancies, obtained by parallax analysis compared with calculated values of z_{CF} , appear to result from the complicated nature of the lateral pressure within the membrane leaflet, especially when the phosphoglyceride chains contain *cis* double bonds (67). Overall, however, the parallax analysis confirms that the Me₄-BODIPY-8 fluorophore is immersed in the apolar bilayer zone at a depth determined by the linking acyl chain and agrees with the conclusion obtained on the basis of free iodide quenching.

In summary, we conclude that Me₄-BODIPY-8-labeled lipids possess attractive photophysical features as membrane probes: longwave emission, high sensitivity, and stability, supplemented with improved residence in the apolar membrane region. Such features endow the Me₄-BODIPY-8 fluorophore with obvious advantages over other fluorophores, such as unsymmetrical, dimethylated BODIPYs, NBD (1), or perylene (5). By embedding in the bilayer to the maximal depth allowed by the linking acyl chain, the Me₄-BODIPY-8 fluorophore is expected to be particularly useful for studies in which fluorophore localization in the membrane is needed (e.g., studies of membrane topography involving protein-lipid interactions). In

such capacity, Me₄-BODIPY-8 probes could be used as fluorescence resonance energy transfer acceptors in combination with pyrenyl-, DPH-, or anthroyloxy-labeled lipids (1). Me₄-BODIPY-8-labeled lipids also are expected to complement existing BODIPY probes used to monitor lipid traffic between cell membrane processes by fluorescence imaging microscopy, because they offer the same advantages of narrow-wavelength emission maximum and high photostability. 

The authors are grateful for support provided by the Russian Foundation for Basic Research (Grant 06-04-48666 to I.A.B. and J.G.M.), the United States Public Health Service (Grants HL-49180 to H.L.B. and GM-45928 to R.E.B.), and the Hormel Foundation. Help with bilayer modeling, given by the Laboratory of Biomolecular Modeling, Institute of Bioorganic Chemistry, Russian Academy of Sciences (www.model.nmr.ru), is also appreciated.

REFERENCES

- Maier, O., V. Oberle, and D. Hoekstra. 2002. Fluorescent lipid probes: some properties and applications. *Chem. Phys. Lipids*. **116**: 3–18.
- Cantor, R. S. 1997. Lateral pressures in cell membranes: a mechanism for modulation of protein function. *J. Phys. Chem.* **101**: 1723–1725.
- White, S. H., A. S. Ladokhin, S. Jayasinghe, and K. Hristova. 2001. How membranes shape protein structure. *J. Biol. Chem.* **276**: 32395–32398.
- Thulborn, K. R., and W. H. Sawyer. 1978. Properties and locations of a set of fluorescent probes sensitive to the fluidity gradient of the lipid bilayer. *Biochim. Biophys. Acta.* **511**: 125–140.
- Bergelson, L. D., J. G. Molotkovsky, and Y. M. Manevich. 1985. Lipid-specific probes in studies of biological membranes. *Chem. Phys. Lipids*. **37**: 165–195.
- Chattopadhyay, A., and E. London. 1987. Parallax method for direct measurement of membrane penetration depth utilizing fluorescence quenching by spin-labeled phospholipids. *Biochemistry*. **26**: 39–45.
- Abrams, F. S., and E. London. 1993. Extension of the parallax analysis of membrane penetration depth to the polar region of model membranes: use of fluorescence quenching by a spin-label attached to the phospholipids polar headgroup. *Biochemistry*. **32**: 10826–10831.
- Treibs, A., and F.H. Kreuzer. 1968. Difluorborol-Komplexe von Di- und Tripyrrylmethenen. *Liebigs Ann. Chem.* **718**: 208–223.
- Johnson, I. D., H. C. Kang, and R. P. Haugland. 1991. Fluorescent membrane probes incorporating dipyrrometheneboron difluoride fluorophores. *Anal. Biochem.* **198**: 228–237.
- Karolin, J., L. B-Å. Johansson, L. Strandberg, and T. Ny. 1994. Fluorescence and absorption spectroscopic properties of dipyrrometheneboron difluoride (BODIPY) derivatives in liquids, lipid membranes, and proteins. *J. Am. Chem. Soc.* **116**: 7801–7806.
- Isaksson, M., S. Kalinin, S. Lobov, T. Ny, and L. B-Å. Johansson. 2003. An environmental-sensitive BODIPY derivative with bio-application: spectral and photophysical properties. *J. Fluorescence*. **13**: 379–384.
- Hendrickson, H. S., E. K. Hendrickson, I. D. Johnson, and S. A. Farber. 1999. Intramolecularly quenched BODIPY-labeled phospholipid analogs in phospholipase A2 and platelet-activating factor acetylhydrolase assays and *in vivo* fluorescence imaging. *Anal. Biochem.* **276**: 27–35.
- Mikhalyov, I. I., and J. G. Molotkovsky. 2003. Synthesis and characteristics of fluorescent BODIPY-labeled gangliosides. *Russ. J. Bioorg. Chem.* **29**: 168–174.
- Michalet, X., A. N. Kapanidis, T. Laurence, F. Pinaud, S. Doose, M. Pflughoeft, and S. Weiss. 2003. The power and prospects of fluorescence microscopies and spectroscopies. *Annu. Rev. Biophys. Biomol. Struct.* **32**: 161–182.
- Invitrogen™. Accessed May 1, 2007, at <http://probes.invitrogen.com>.
- Menger, F. M., J. S. Keiper, and K. L. Caran. 2002. Depth-profiling with giant vesicle membranes. *J. Am. Chem. Soc.* **116**: 7801–7806.
- Kaiser, R. D., and E. London. 1998. Determination of the depth of BODIPY probes in model membranes by parallax analysis of fluorescence quenching. *Biochim. Biophys. Acta.* **1375**: 13–22.
- Pagano, R. E., and C. S. Chen. 1998. Use of BODIPY-labeled sphingolipids to study membrane traffic along the endocytic pathway. *Ann. N. Y. Acad. Sci.* **845**: 152–160.
- Bergström, F., I. Mikhalyov, P. Häggglöf, R. Wortmann, T. Ny, and L. B-Å. Johansson. 2002. Dimers of dipyrrometheneboron difluoride (BODIPY) with light spectroscopic applications in chemistry and biology. *J. Am. Chem. Soc.* **124**: 196–204.
- Boldyrev, I. A., and J. G. Molotkovsky. 2006. A synthesis and properties of new 4,4-difluoro-3a,4a-diaza-s-indacene (BODIPY)-labeled lipids. *Russ. J. Bioorg. Chem.* **32**: 87–92.
- Omelkov, A. V., Y. B. Pavlova, I. A. Boldyrev, and J. G. Molotkovsky. 2007. Depth-dependent investigation of apolar zone of the lipid membranes with the help of a set of fluorescent probes, Me₄-BODIPY-8-labeled phosphatidylcholines. *Russ. J. Bioorg. Chem.* **33**: In press.
- Vodovozova, E. L., E. V. Moiseeva, G. K. Grechko, G. P. Gayenko, N. E. Nifantev, N. V. Bovin, and J. G. Molotkovsky. 2001. Antitumor activity of cytotoxic liposomes equipped with selectin ligand SiaLex, in a mouse mammary adenocarcinoma model. *Eur. J. Cancer.* **36**: 942–949.
- Ladokhin, A. S., S. Jayasinghe, and S. H. White. 2000. How to measure and analyze tryptophan fluorescence in membranes properly, and why bother? *Anal. Biochem.* **285**: 235–245.
- Kalinin, S. V., and J. G. Molotkovsky. 2001. Anion binding to lipid bilayers: A study using fluorescent lipid probes. *Membr. Cell Biol.* **14**: 831–846.
- Li, X-M., M. Malakhova, X. Lin, H. M. Pike, T. Chung, J. G. Molotkovsky, and R. E. Brown. 2004. Human glycolipid transfer protein: probing conformation using fluorescence spectroscopy. *Biochemistry*. **43**: 10285–10294.
- White, G., J. Pencer, B. G. Nickel, J. M. Wood, and F. R. Hallett. 1996. Optical changes in unilamellar vesicles experiencing osmotic stress. *Biophys. J.* **71**: 2701–2715.
- Matsuzaki, K., O. Murase, K. Sugishita, S. Yoneyama, K. Akada, M. Ueha, A. Nakamura, and S. Kobayashi. 2000. Optical characterization of liposomes by right angle light scattering and turbidity measurement. *Biochim. Biophys. Acta.* **1467**: 219–226.
- Chattopadhyay, A., and E. London. 1987. Parallax method for direct measurement of membrane penetration depth utilizing fluorescence quenching by spin-labeled phospholipids. *Biochemistry*. **26**: 39–45.
- Heller, H., M. Schäfer, and K. Schulten. 1993. Molecular dynamics simulation of a bilayer of 200 lipids in the gel and in the liquid-crystal phases. *J. Phys. Chem.* **97**: 8343–8360.
- Smaby, J. M., and H. L. Brockman. 1990. Surface dipole moments of lipids at the argon-water interface: similarities among glycerol-ester-based lipids. *Biophys. J.* **58**: 195–204.
- Momsen, W. E., J. M. Smaby, and H. L. Brockman. 1990. The suitability of nichrome for measurement of gas-liquid interfacial tension by the Wilhelmy method. *J. Colloid Interface Sci.* **135**: 547–552.
- Dahim, M., N. K. Mizuno, X-M. Li, W. E. Momsen, M. M. Momsen, and H. L. Brockman. 2002. Physical and photophysical characterization of a BODIPY phosphatidylcholine as a membrane probe. *Biophys. J.* **83**: 1511–1524.
- Brockman, H. L. 1994. Dipole potential of lipid membranes. *Chem. Phys. Lipids*. **73**: 57–79.
- Brockman, H. L., K. R. Applegate, M. M. Momsen, W. C. King, and J. A. Glomset. 2003. Packing and electrostatic behavior of *sn*-2-docosahexaenoyl and -arachidonoyl phosphoglycerides. *Biophys. J.* **85**: 2384–2396.
- Davies, J. T., and E. K. Rideal. 1963. *Interfacial Phenomena*. 2nd edition. Academic Press, New York.
- Needham, D. 1995. Cohesion and permeability of lipid bilayer vesicles. In *Permeability and Stability of Lipid Bilayers*. E. A. DiSalvo and S. A. Simon, editors. CRC Press, Boca Raton, FL. 49–76.
- Behroozi, F. 1996. Theory of elasticity in two dimensions and its application to Langmuir-Boldgett films. *Langmuir*. **12**: 2289–2291.
- Brown, R. E., and H. L. Brockman. 2007. Using monomolecular films to characterize lipid lateral interactions. *Methods Mol. Biol.* **398**: 41–58.

39. Smaby, J. M., M. M. Momsen, H. L. Brockman, and R. E. Brown. 1997. Phosphatidylcholine acyl unsaturation modulates the decrease in interfacial elasticity induced by cholesterol. *Biophys. J.* **73**: 1492–1505.
40. Li, X-M., M. M. Momsen, J. M. Smaby, H. L. Brockman, and R. E. Brown. 2003. Sterol structure and sphingomyelin acyl chain length modulate lateral packing elasticity and detergent solubility in model membranes. *Biophys. J.* **85**: 3788–3801.
41. Zhai, X., X-M. Li, M. M. Momsen, H. L. Brockman, and R. E. Brown. 2006. Lactosylceramide: lateral interactions with cholesterol. *Biophys. J.* **91**: 2490–2500.
42. Smaby, J. M., H. L. Brockman, and R. E. Brown. 1994. Cholesterol's interfacial interactions with sphingomyelins and phosphatidylcholines: hydrocarbon chain structure determines the magnitude of condensation. *Biochemistry*. **31**: 9135–9142.
43. Smaby, J. M., M. Momsen, V. S. Kulkarni, and R. E. Brown. 1996. Cholesterol-induced interfacial area condensations of galactosylceramides and sphingomyelins with identical acyl chains. *Biochemistry*. **35**: 5696–5704.
44. Burghart, A., H. Kim, M. B. Welch, L. H. Thoresen, J. Reibenspies, K. Burgess, F. Bergström, and L. B-Å. Johansson. 1999. 3,5-Diaryl-4,4-difluoro-4-bora-3a,4a-diaza-s-indacene (BODIPY) dyes: synthesis, spectroscopic, electrochemical, and structural properties. *J. Org. Chem.* **64**: 7813–7819.
45. Burghardt, T. P., J. E. Lyke, and K. Ajtai. 1996. Fluorescence emission and anisotropy from rhodamine dimers. *Biophys. Chem.* **59**: 119–131.
46. Chalpin, D. B., and A. M. Kleinfeld. 1983. Interaction of fluorescence quenchers with the *n*-(9-anthroxyl) fatty acid membrane probes. *Biochim. Biophys. Acta.* **731**: 465–474.
47. Liu, L-P., and C. M. Deber. 1997. Anionic phospholipids modulate peptide insertion into membranes. *Biochemistry*. **36**: 5476–5482.
48. Subbarao, N. K., and R. C. MacDonald. 1993. Experimental method to correct fluorescence intensities for the inner filter effect. *Analyst.* **118**: 913–916.
49. Lagane, B., S. Mazères, C. Le Grimellec, L. Cézanne, and A. Lopez. 2002. Lateral distribution of cholesterol in membranes probed by means of a pyrene-labelled cholesterol: effect of acyl chain unsaturation. *Biophys. Chem.* **95**: 7–22.
50. Lakowicz, J. R. 1999. Principles of Fluorescent Spectroscopy. Kluwer Academic/Plenum Press, New York.
51. Birks, J. B. 1970. Photophysical processes. In *Photophysics of Aromatic Molecules*. J. B. Birks, editor. Wiley-Interscience, London. 29–43.
52. Birks, J. B. 1975. Excimers. *Rep. Prog. Phys.* **38**: 903–974.
53. Birks, J. B. 1975. The photophysics of aromatic excimers. In *The Exciplex*. M. Gordon and W. R. Ware, editors. Academic Press, New York. 39–73.
54. Mikhalyov, I., N. Gretskeya, F. Bergsröm, and L. B-Å. Johansson. 2002. Electronic ground and excited state properties of dipyrrometheneboron difluoride (BODIPY): dimers with application to biosciences. *Phys. Chem. Chem. Phys.* **4**: 5663–5670.
55. Cadenhead, D. A., B. M. J. Kellner, and F. Miller-Landau. 1975. A comparison of a spin-label and a fluorescent cell membrane probe using pure and mixed monomolecular films. *Biochim. Biophys. Acta.* **382**: 253–259.
56. Lee, T. D., G. B. Birrell, and J. F. W. Keana. 1978. A new series of minimum steric perturbation nitroxide lipid spin probes. *J. Am. Chem. Soc.* **100**: 1618–1619.
57. Vogel, A., H. A. Scheidt, and D. Huster. 2003. The distribution of lipid attached spin probes in bilayers: application to membrane protein topology. *Biophys. J.* **85**: 1691–1701.
58. Cranney, M., R. B. Cundall, G. R. Jones, J. T. Richards, and E. W. Thomas. 1983. Fluorescence lifetime and quenching studies on some interesting diphenylhexatriene membrane probes. *Biochim. Biophys. Acta.* **735**: 418–425.
59. Langner, M., and S. W. Hui. 1991. Iodide penetration into lipid bilayer as a probe of membrane lipid organization. *Chem. Phys. Lipids.* **60**: 127–132.
60. Barenholz, Y., T. Cohen, R. Korenstein, and M. Ottolenghi. 1991. Organization and dynamics of pyrene and pyrene lipids in intact lipid bilayers. Photo-induced charge transfer processes. *Biophys. J.* **59**: 110–124.
61. Marsh, D. 2002. Membrane water-penetration profiles from spin labels. *Eur. Biophys. J.* **31**: 559–562.
62. Blatt, E., and W. H. Sawyer. 1985. Depth-dependent fluorescent quenching in micelles and membranes. *Biochim. Biophys. Acta.* **822**: 43–62.
63. Sankaram, M. B., and T. E. Thompson. 1990. Modulation of phospholipid acyl chain order by cholesterol. A solid-state ²H nuclear magnetic resonance study. *Biochemistry.* **29**: 10676–10684.
64. Molotkovsky, J. G., M. O. Karyukhina, and L. D. Bergelson. 1987. A fluorescence method for studying bilayer membrane water permeability. *Biol. Membr. (Engl. Transl.)*. **4**: 387–394.
65. Marsh, D. 2001. Polarity and permeation profiles in lipid membranes. *Proc. Natl. Acad. Sci. USA.* **98**: 7777–7782.
66. Eftink, M. R., and C. A. Ghiron. 1981. Fluorescence quenching studies with proteins. *Anal. Biochem.* **114**: 199–227.
67. Templer, R. H., S. J. Castle, A. R. Curran, G. Rumbles, and D. R. Klug. 1998. Sensing isothermal changes in the lateral pressure in model membranes using di-pyrenyl phosphatidylcholine. *Faraday Discuss.* **111**: 41–53.

ERRATA

In the article “New BODIPY lipid probes for fluorescence studies of membranes,” by Boldyrev et al., published in the July 2007 issue of the *Journal of Lipid Research* (Volume 48, pages 1518–1532), Figure 6D and its legend contained errors. Figure 6 and its legend should read:

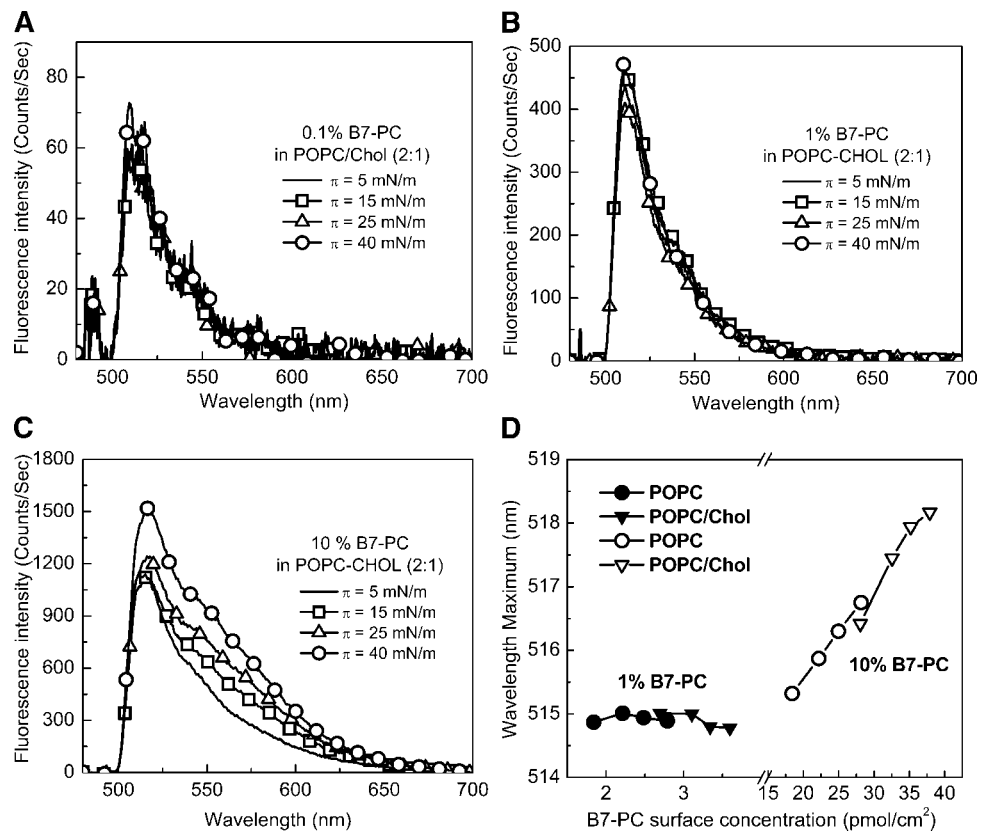


Fig. 6. Fluorescence emission response of POPC/cholesterol (Chol) mixed monolayers containing B7-PC. A–C: Fluorescence emission spectra of POPC/Chol (2:1) monolayers containing B7-PC mixed at mole fractions of 0.001 (A), 0.01 (B), and 0.1 (C) at surface pressures of 5 mN/m (lines lacking symbols), 15 mN/m (lines marked by squares), 25 mN/m (lines marked by triangles), and 40 mN/m (lines marked by circles). D: Emission wavelength maximum as a function of B7-PC surface concentration in POPC and POPC/Chol (2:1) monolayers. B7-PC mole fractions of 0.01 (filled symbols) and 0.1 (unfilled symbols) mixed with either POPC (circles) or POPC/Chol (2:1) (triangles) are shown at surface pressures of 5, 15, 25, and 40 mN/m, with the highest surface pressure corresponding to the highest wavelength maximum.